

(d) The calculation shows that substantial information about dislocation geometry can be obtained from a distorted [001] Tanaka pattern. In some cases this allows the dislocation to be identified uniquely. In general a unique determination of geometric properties needs an extra two-beam image.

(e) The advantage of this method is that the projection of **u** and **b** can be directly observed during TEM observation. This is good for *in situ* investigation. Its disadvantages are that it requires observations at a special orientation (a $\langle 001 \rangle$ axis) and that it may not be applied to materials where there is no square-like ZOLZ pattern in a perfect area.

The authors are grateful to Professor Z. Zhou of Beijing Science and Technology for helpful discussions. Mr X. G. Zhang and Mrs K. P. Xu of the Institute of Anshan Iron and Steel Research and Mrs A. X. Li of Shenyang Institute of Metal Research are thanked for assistance in deforming crystals. GL thanks the National Postdoctoral Committee of China for the postdoctoral fellowship.

Acta Cryst. (1990). **A46**, 112–123

Extinction in Finite Perfect Crystals: Case of a Sphere

BY M. AL HADDAD* AND P. BECKER†

*Laboratoire de Cristallographie, associé à l'Université J. Fourier, CNRS, 166X,
38042 Grenoble CEDEX, France*

(Received 6 December 1988; accepted 7 September 1989)

Abstract

The extinction factor in finite perfect crystals is calculated from pure dynamical theory. In particular, a detailed solution is proposed for a sphere, in which case the extinction factor depends on the Bragg angle θ and the parameter (R/Λ) , where R is the radius of the crystal and Λ the extinction length. An approximate solution based on the Laue geometry is proposed and corrections to take care of the complex boundary conditions are presented. An expression easily usable in refinement programs is proposed that fits the exact value to better than 1%.

Introduction

Two main difficulties are encountered when developing a model for extinction. The major one is to decide

* Present address: Atomic Energy Commission, PO Box 6091, Damascus, Syria.

† Present address: Laboratoire de Minéralogie-Cristallographie, Université Pierre et Marie Curie, Tour 16, 4 Place Jussieu, 75252 Paris CEDEX 05, France.

References

- BIAN, W. M. (1986). *J. Chin. Electron Microsc. Soc.* **5**, No. 3, 46. (In Chinese.)
- CARPENTER, R. W. & SPENCE, J. C. H. (1982). *Acta Cryst.* **A38**, 55–61.
- CHERNS, D., KIELY, C. J. & PRESTON, A. R. (1988). *Ultramicroscopy*, **24**, 355–369.
- CHERNS, D. & PRESTON, A. R. (1986). Proc. XIth Int. Congr. on Electron Microscopy, Kyoto, Japan, pp. 721–722.
- COWLEY, J. M. (1981). *Diffraction Physics*, p. 196. Amsterdam: North-Holland.
- HEAD, A. K., HUMBLE, P., CLAREBROUGH, L. M., MORTON, A. J. & FORWOOD, C. T. (1973). *Computed Electron Micrographs and Defect Identification*. Amsterdam: North-Holland.
- HIRSCH, P. B., HOWIE, A., NICHOLSON, R. B., PASHLEY, D. W. & WHELAN, M. J. (1977). *Electron Microscopy of Thin Crystals*, Ch. 9. New York: Robert E. Krieger.
- HIRTH, J. P. & LOTHE, J. (1980). *Theory of Dislocations*, 2nd ed., p. 282. New York: John Wiley.
- RAY, I. L. F. & COCKAYNE, D. J. H. (1970). *Philos. Mag.* **22**, 853–856.
- STROH, A. N. (1958). *Philos. Mag.* **3**, 625–646.
- TANAKA, M., SAITO, R., UENO, K. & HARADA, Y. (1980). *J. Electron Microsc.* **29**, 408–412.
- TANAKA, M., TERAUCHI, M. & KANEYAMA, T. (1988). *Convergent-Beam Electron Diffraction II*. Tokyo: JEOL-Maruzen.
- WEN, J., WANG, R. & LU, G. (1989). *Acta Cryst.* **A45**, 422–427.

on a coupling scheme between coherent and incoherent contributions to the diffracted intensity. A model based on purely incoherent intensities has been developed by Becker & Coppens (1974, 1975), which essentially corresponds to the assumption of pure 'secondary extinction'. To go beyond this approach, Kato (1980) developed a statistical dynamical theory for the propagation of X-rays or neutrons in a distorted crystal. In this new approach, the separation between coherent and incoherent components of the intensity is rather subtle, which shows that 'secondary' and 'primary' extinction are not independent concepts and that the celebrated mosaic model is invalid. The present authors have reformulated Kato's ideas in a more general way (Al Haddad & Becker, 1988; Becker & Al Haddad, 1989, 1990; see also Guigay, 1989). This statistical theory contains the purely incoherent coupling as one limiting case. At the other limit, one also retrieves the purely coherent or dynamical theory that corresponds to 'primary extinction by a perfect crystal'.

The second difficulty has to do with the geometrical boundaries imposed by the sample under study. All

known propagation equations have a well defined solution for an infinite parallel plate in transmission geometry. Most crystals under study in X-ray or neutron crystallography have a rather regular shape, leading to very intricate boundary conditions. A useful approach consists in approximating the sample by a sphere, and then introducing some modifications to take the anisotropy of the crystal shape into account (Becker & Coppens, 1974, 1975). The detailed solution for a polyhedral sample has also been considered (Becker & Dunstetter, 1984) and the validity of simple geometrical approximations was discussed.

In the present paper, we intend to solve the case of a perfect crystal for an isotropic sample approximated by a sphere. The geometrical boundary will thus be the essential difficulty in studying the propagation of the wave fields in the incident and diffracted directions.

Propagation equations, boundary conditions, extinction factor

In Fig. 1, we present the geometry of scattering in a plane that is a section of the crystal.

The portion of the crystal excited by the incident beam in the \mathbf{u}_0 direction is curve ACB . The portion where the diffracted beam (\mathbf{u}_h direction) exits is curve DBC . The entrance and exit surfaces overlap by the portion CB , and this is the cause of the difficulties due to the boundary. Let S be a point on the entrance surface and M a point on the exit surface. To the couple (S, M) is associated a unique point m and we define the two optical path lengths, s_0 and s_h , as $s_0 = \overline{Sm}$, $s_h = \overline{mM}$. s_0 and s_h are therefore coordinates along the axes \mathbf{u}_0 and \mathbf{u}_h .

Let D_0 and D_h be the amplitudes of the waves propagating along the incident and diffracted directions, respectively. In the case of a perfect crystal, in the two-beam case, the propagation is governed by Takagi-Taupin equations (Kato, 1973, 1976).

$$\frac{\partial D_0}{\partial s_0} = i\chi_{\bar{h}}D_h, \quad \frac{\partial D_h}{\partial s_h} = i\chi_h D_0, \quad (1)$$

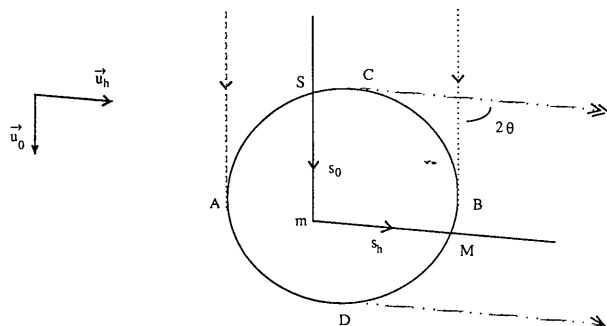


Fig. 1. Geometry of the scattering $\overline{Sm} = s_0$, $\overline{mM} = s_h$.

where for neutrons:

$$\chi_h = (\lambda/V)aF(\mathbf{h}), \quad \chi_{\bar{h}} = (\lambda/V)aF(-\mathbf{h}) \quad (2)$$

$$a = 10^{-12} \text{ cm};$$

and for X-rays:

$$\chi_h = (\lambda/V)r_0CF(\mathbf{h}), \quad \chi_{\bar{h}} = (\lambda/V)r_0CF(-\mathbf{h}), \quad (3)$$

with F the structure factor, λ the wavelength, V the unit-cell volume, r_0 the classical radius of the electron and C the polarization factor. Notice that the coefficients χ_h and $\chi_{\bar{h}}$ are not the Fourier coefficients of the microscopic susceptibility.

The following strategy has been proposed to solve (1) for a given sample (Kato, 1976; Becker, 1977a, b; Becker & Dunstetter, 1984).

One first considers the scattering originating from a point source S on the entrance surface ACB , with unit intensity. The incident beam is thus characterized by

$$D_0^0 = \delta(s_h). \quad (4)$$

One then calculates the diffracted intensity $I_h(S \rightarrow M)$ at the exit point M , originating from S . The couple (S, M) of points can be replaced by a point m within the 'extended' domain $AEDBCA$, defined in Fig. 2.

One can show (Kato, 1976; Becker, 1977b), for a crystal illuminated by a homogeneous beam or a plane wave, that the integrated diffracted power is given by

$$P = (\lambda/\sin 2\theta) \int_{v'} dv_m I_h(m) \quad (5)$$

where

$$I_h(m) = I_h(S \rightarrow M) = |D_h(m)|^2. \quad (6)$$

Equation (5) is obtained by varying the exit and entrance points successively.

In the kinematic approximation (simple scattering), the diffracted power becomes

$$P_k = (\lambda/\sin 2\theta)|\chi_h|^2 v, \quad (7)$$

where v is the volume of the crystal.

The extinction factor is defined by

$$P = P_k y \quad (8)$$

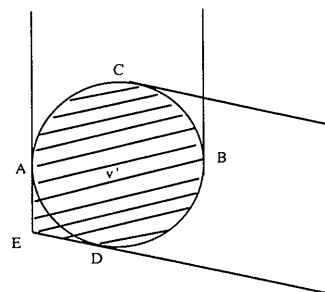


Fig. 2. Definition of the volume v' for variation of m shown as the shaded domain $AEDBC$.

and, for a perfect finite crystal, y is normally given by

$$y = (1/|\chi_h|^2 v) \int_{v'} dv_m I_h(m). \quad (9)$$

In the general case of an absorbing crystal, $\chi_{\bar{h}} \neq \chi_h^*$, which leads to anomalous scattering and anomalous absorption. We will not consider this case here, and we will devote our efforts to the case of a perfect non-absorbing crystal.

Approximate solution in the Laue approximation

In order to evaluate (5) or (9), it is necessary to obtain $D_h(m)$ for any point m within the domain v' . Three basic configurations can be encountered, shown in Fig. 3.

In the case of configuration I, the entire parallelogram $SmMm'$ belongs to the crystal: it is the pure Laue case. In contrast, for configurations II and III, $SmMm'$ has a finite intersection with the crystal surface and this corresponds to a mixed Laue-Bragg situation.

It has been shown (Becker & Dunstetter, 1974) that, for small scattering angles, case I is the only relevant situation. The corrections due to cases II and III only become important for large angles of diffraction. The problem has been discussed by Kawamura & Kato (1983) and Becker & Dunstetter (1984): taking cases II and III into account is possible, but leads to complicated calculations. Most applications of extinction theories have been restricted to approximations which discard configurations like II and III. In this paper, we shall start by developing the same kind of approximation and we shall later consider the corrections implied by a more exact treatment.

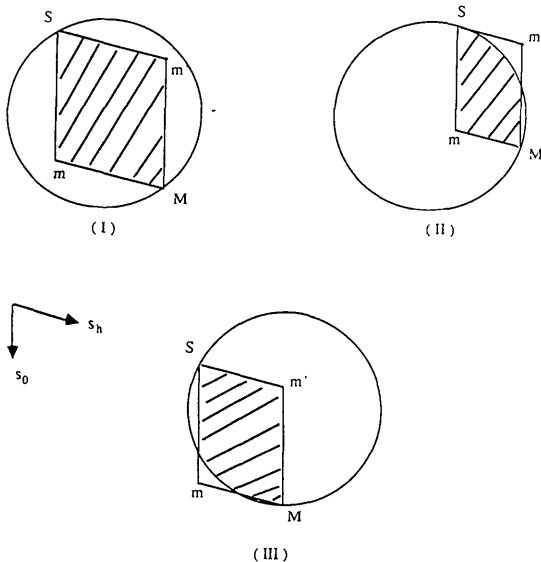


Fig. 3. The three basic geometrical configurations for scattering.

In this section, we therefore assume that I is the only situation and therefore we must replace v' by the crystal volume v .

Solving (1) with the boundary condition (4), one gets

$$D_h = i\chi_h J_0[2\chi(s_0 s_h)^{1/2}] \quad (10)$$

where $\chi^2 = \chi_h \chi_{\bar{h}}$ and J_0 is a zero-order Bessel function. The extinction factor is

$$y_p = (1/v) \int_v |J_0[2\chi(s_0 s_h)^{1/2}]|^2 dv \quad (11)$$

for a non-absorbing crystal.

In the case of a sphere of radius R , we define the parameter

$$x = R\chi = R/\Lambda. \quad (12)$$

One gets

$$y_p = (3/4\pi) \int_{R=1} |J_0[2x(s_0 s_h)^{1/2}]|^2 dv, \quad (13)$$

where the integral is now over a sphere of unit radius. Equation (13) is computed, for each x and θ , by a Gaussian quadrature with 16 points in each dimension. The results for $1/y_p$ versus x , for different values of $\sin \theta$, are shown in Fig. 4, and numerical values are given in Table 1. y_p must be invariant by an interchange of $(\mathbf{u}_0, \mathbf{u}_h)$ into $(-\mathbf{u}_h, -\mathbf{u}_0)$; therefore, y_p is an even function of $\sin \theta$. The variation of y_p with $\sin \theta$, for a fixed x , is shown in Fig. 5.

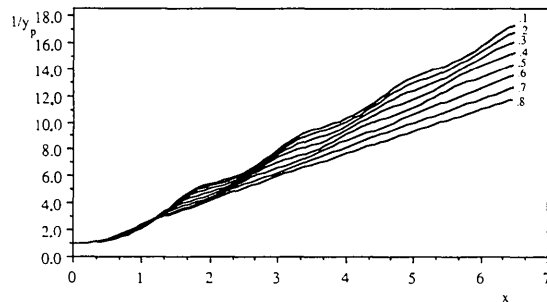


Fig. 4. $1/y_p$ as a function of x , for different $\sin \theta$ values.

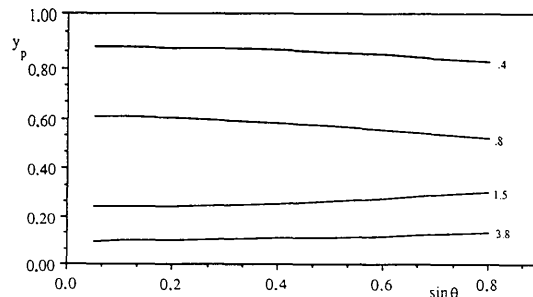


Fig. 5. $y_p(\sin \theta)$ for different values of x .

Table 1. $y_p(x, \sin \theta)$ as the result of Gaussian integration

sin q	0.05	0.1	0.2	0.3	0.4	0.5	0.6	0.7	0.8
X									
0.0	1.0000	1.0000	1.0000	1.0000	1.0000	1.0000	1.0000	1.0000	1.0000
0.1	0.9920	0.9920	0.9918	0.9915	0.9911	0.9905	0.9898	0.9888	0.9876
0.2	0.9685	0.9683	0.9677	0.9666	0.9650	0.9627	0.9598	0.9561	0.9516
0.3	0.9306	0.9303	0.9289	0.9266	0.9231	0.9185	0.9124	0.9049	0.8957
0.4	0.8803	0.8797	0.8775	0.8737	0.8681	0.8605	0.8510	0.8393	0.8254
0.5	0.8199	0.8191	0.8160	0.8106	0.8028	0.7926	0.7798	0.7647	0.7472
0.6	0.7524	0.7514	0.7474	0.7407	0.7310	0.7186	0.7036	0.6864	0.6674
0.7	0.6808	0.6796	0.6750	0.6671	0.6563	0.6427	0.6269	0.6096	0.5917
0.8	0.6080	0.6067	0.6017	0.5934	0.5821	0.5686	0.5537	0.5386	0.5242
0.9	0.5369	0.5356	0.5306	0.5224	0.5117	0.4995	0.4872	0.4762	0.4672
1.0	0.4700	0.4687	0.4640	0.4566	0.4474	0.4379	0.4297	0.4240	0.4212
1.1	0.4091	0.4080	0.4040	0.3979	0.3911	0.3853	0.3820	0.3821	0.3853
1.2	0.3556	0.3548	0.3517	0.3475	0.3437	0.3422	0.3442	0.3497	0.3576
1.3	0.3104	0.3098	0.3079	0.3059	0.3054	0.3083	0.3152	0.3250	0.3359
1.4	0.2734	0.2732	0.2726	0.2729	0.2758	0.2828	0.2935	0.3061	0.3180
1.5	0.2445	0.2445	0.2452	0.2478	0.2538	0.2641	0.2773	0.2909	0.3022
1.6	0.2227	0.2230	0.2249	0.2294	0.2380	0.2505	0.2648	0.2777	0.2874
1.7	0.2069	0.2075	0.2104	0.2165	0.2268	0.2404	0.2543	0.2654	0.2733
1.8	0.1959	0.1967	0.2003	0.2075	0.2188	0.2322	0.2445	0.2534	0.2598
1.9	0.1883	0.1893	0.1933	0.2011	0.2124	0.2248	0.2348	0.2415	0.2472
2.0	0.1830	0.1839	0.1881	0.1959	0.2066	0.2172	0.2247	0.2298	0.2357
2.1	0.1787	0.1796	0.1837	0.1911	0.2007	0.2090	0.2143	0.2187	0.2255
2.2	0.1746	0.1755	0.1793	0.1860	0.1940	0.2002	0.2039	0.2086	0.2166
2.3	0.1702	0.1709	0.1743	0.1801	0.1866	0.1909	0.1940	0.1996	0.2087
2.4	0.1650	0.1657	0.1686	0.1735	0.1785	0.1816	0.1849	0.1919	0.2017
2.5	0.1591	0.1596	0.1621	0.1662	0.1701	0.1726	0.1768	0.1853	0.1953
2.6	0.1525	0.1529	0.1550	0.1585	0.1617	0.1644	0.1700	0.1795	0.1891
2.7	0.1455	0.1459	0.1477	0.1509	0.1538	0.1571	0.1643	0.1743	0.1831
2.8	0.1384	0.1387	0.1405	0.1435	0.1466	0.1511	0.1595	0.1693	0.1772
2.9	0.1315	0.1318	0.1336	0.1369	0.1404	0.1461	0.1554	0.1645	0.1717
3.0	0.1251	0.1255	0.1275	0.1310	0.1353	0.1421	0.1516	0.1596	0.1664
3.1	0.1195	0.1199	0.1222	0.1262	0.1311	0.1387	0.1478	0.1547	0.1616
3.2	0.1147	0.1153	0.1178	0.1222	0.1277	0.1358	0.1440	0.1500	0.1572
3.3	0.1109	0.1115	0.1143	0.1190	0.1250	0.1330	0.1400	0.1455	0.1532
3.4	0.1078	0.1085	0.1116	0.1165	0.1226	0.1301	0.1359	0.1413	0.1495
3.5	0.1054	0.1061	0.1094	0.1143	0.1202	0.1269	0.1318	0.1375	0.1460
3.6	0.1035	0.1042	0.1075	0.1122	0.1178	0.1236	0.1278	0.1341	0.1426
3.7	0.1018	0.1025	0.1057	0.1102	0.1152	0.1200	0.1240	0.1310	0.1393
3.8	0.1002	0.1008	0.1038	0.1079	0.1123	0.1164	0.1206	0.1282	0.1360
3.9	0.0984	0.0990	0.1018	0.1054	0.1093	0.1128	0.1177	0.1255	0.1328
4.0	0.0965	0.0970	0.0995	0.1027	0.1061	0.1094	0.1151	0.1228	0.1298
4.1	0.0943	0.0948	0.0970	0.0998	0.1029	0.1064	0.1128	0.1201	0.1270
4.2	0.0919	0.0923	0.0943	0.0968	0.0999	0.1038	0.1107	0.1175	0.1243
4.3	0.0893	0.0897	0.0916	0.0939	0.0971	0.1015	0.1087	0.1148	0.1219
4.4	0.0866	0.0870	0.0888	0.0912	0.0946	0.0996	0.1067	0.1122	0.1195
4.5	0.0840	0.0844	0.0862	0.0887	0.0925	0.0979	0.1046	0.1098	0.1173
4.6	0.0815	0.0819	0.0838	0.0865	0.0906	0.0964	0.1024	0.1076	0.1151
4.7	0.0793	0.0797	0.0817	0.0847	0.0891	0.0948	0.1002	0.1056	0.1129
4.8	0.0773	0.0778	0.0799	0.0832	0.0877	0.0933	0.0979	0.1037	0.1108
4.9	0.0756	0.0761	0.0784	0.0818	0.0864	0.0916	0.0957	0.1020	0.1088
5.0	0.0743	0.0748	0.0772	0.0807	0.0851	0.0898	0.0937	0.1003	0.1069
5.1	0.0731	0.0737	0.0761	0.0796	0.0837	0.0879	0.0918	0.0987	0.1050
5.2	0.0721	0.0727	0.0751	0.0785	0.0822	0.0859	0.0902	0.0970	0.1032
5.3	0.0712	0.0718	0.0741	0.0773	0.0806	0.0840	0.0887	0.0954	0.1016
5.4	0.0703	0.0708	0.0731	0.0760	0.0789	0.0822	0.0874	0.0937	0.0999
5.5	0.0694	0.0699	0.0719	0.0746	0.0772	0.0806	0.0862	0.0920	0.0983
5.6	0.0683	0.0688	0.0707	0.0730	0.0755	0.0791	0.0850	0.0905	0.0968
5.7	0.0672	0.0676	0.0693	0.0715	0.0739	0.0778	0.0837	0.0890	0.0952
5.8	0.0659	0.0663	0.0679	0.0699	0.0724	0.0767	0.0824	0.0876	0.0937
5.9	0.0646	0.0649	0.0664	0.0684	0.0711	0.0757	0.0811	0.0863	0.0922
6.0	0.0632	0.0635	0.0650	0.0670	0.0699	0.0747	0.0797	0.0850	0.0908
6.1	0.0618	0.0621	0.0637	0.0657	0.0689	0.0738	0.0783	0.0838	0.0895
6.2	0.0605	0.0608	0.0624	0.0646	0.0680	0.0728	0.0770	0.0826	0.0882
6.3	0.0594	0.0597	0.0614	0.0637	0.0672	0.0717	0.0758	0.0814	0.0870
6.4	0.0583	0.0586	0.0604	0.0628	0.0664	0.0706	0.0747	0.0802	0.0859
6.5	0.0574	0.0577	0.0596	0.0620	0.0655	0.0694	0.0736	0.0789	0.0848

Table 2. Z_0, Z_1, Z_2 as functions of x

X	Z_0	Z_1	Z_2	X	Z_0	Z_1	Z_2
0.0	1.0000	0.0000	0.0000	3.3	0.1112	0.0888	-0.0323
0.1	0.9922	-0.0055	-0.0024	3.4	0.1085	0.0857	-0.0308
0.2	0.9687	-0.0214	-0.0080	3.5	0.1065	0.0805	-0.0270
0.3	0.9309	-0.0463	-0.0132	3.6	0.1047	0.0740	-0.0217
0.4	0.8807	-0.0776	-0.0132	3.7	0.1030	0.0672	-0.0159
0.5	0.8206	-0.1113	-0.0044	3.8	0.1012	0.0610	-0.0104
0.6	0.7532	-0.1427	0.0143	3.9	0.0992	0.0563	-0.0061
0.7	0.6816	-0.1661	0.0406	4.0	0.0970	0.0533	-0.0034
0.8	0.6086	-0.1766	0.0693	4.1	0.0945	0.0523	-0.0025
0.9	0.5371	-0.1706	0.0935	4.2	0.0918	0.0529	-0.0032
1.0	0.4694	-0.1465	0.1065	4.3	0.0890	0.0546	-0.0051
1.1	0.4076	-0.1060	0.1038	4.4	0.0863	0.0571	-0.0078
1.2	0.3532	-0.0532	0.0847	4.5	0.0837	0.0595	-0.0105
1.3	0.3072	0.0054	0.0519	4.6	0.0813	0.0615	-0.0129
1.4	0.2698	0.0625	0.0112	4.7	0.0792	0.0627	-0.0146
1.5	0.2408	0.1111	-0.0300	4.8	0.0775	0.0628	-0.0154
1.6	0.2195	0.1460	-0.0647	4.9	0.0760	0.0619	-0.0152
1.7	0.2046	0.1647	-0.0877	5.0	0.0748	0.0601	-0.0141
1.8	0.1948	0.1674	-0.0967	5.1	0.0737	0.0577	-0.0124
1.9	0.1884	0.1566	-0.0924	5.2	0.0727	0.0549	-0.0103
2.0	0.1841	0.1367	-0.0778	5.3	0.0717	0.0523	-0.0082
2.1	0.1805	0.1127	-0.0574	5.4	0.0707	0.0500	-0.0063
2.2	0.1767	0.0893	-0.0359	5.5	0.0696	0.0483	-0.0050
2.3	0.1722	0.0701	-0.0170	5.6	0.0684	0.0472	-0.0043
2.4	0.1666	0.0570	-0.0033	5.7	0.0671	0.0469	-0.0042
2.5	0.1600	0.0509	0.0041	5.8	0.0657	0.0471	-0.0047
2.6	0.1527	0.0510	0.0054	5.9	0.0643	0.0477	-0.0055
2.7	0.1451	0.0559	0.0019	6.0	0.0629	0.0485	-0.0065
2.8	0.1376	0.0636	-0.0047	6.1	0.0617	0.0491	-0.0075
2.9	0.1306	0.0723	-0.0128	6.2	0.0605	0.0495	-0.0082
3.0	0.1243	0.0802	-0.0207	6.3	0.0594	0.0494	-0.0085
3.1	0.1189	0.0860	-0.0271	6.4	0.0585	0.0489	-0.0084
3.2	0.1146	0.0889	-0.0311	6.5	0.0577	0.0479	-0.0079

We conclude that the variation with θ is smooth, which suggests the expansion

$$y_p = y_0(x) + \sin^2(\theta)y_1(x) + \sin^4(\theta)y_2(x) + \dots \quad (14)$$

It can be shown by lengthy but elementary algebra that

$$y_0(x) = \frac{3}{2} \left\{ \int_0^1 J_0(4xt) dt - \int_0^1 t^2 J_0(4xt) dt \right\} \quad (15)$$

$$y_1(x) = 6x^2 \left\{ \int_0^1 [t^2 - t^4 + 2t^2 \ln t] J_0(4xt) dt \right\},$$

the expression for y_2 being more complicated.

If the expansion is limited to order 4 in $\sin \theta$, the relative error in y_p can be of the order of 3 to 5% for large x and $\sin \theta$ values. It therefore seems more appropriate to fit $y_p(x, \sin \theta)$ by the expression

$$Z(x, \sin \theta) = Z_0(x) + \sin^2(\theta)Z_1(x) + \sin^4(\theta)Z_2(x), \quad (16)$$

where Z_0, Z_1, Z_2 are obtained numerically, for a given x , by a least-squares fit over $\sin \theta$ values. For

$x < 8$ and $\sin \theta < 0.8$, the relative error $|(y_p - Z)/y_p|$ is always smaller than 1%.

Moreover, $Z_0(x)$ is equal to $y_0(x)$. The functions Z_0, Z_1, Z_2 are tabulated in Table 2, and their variation with x is shown in Fig. 6.

Equation (16) is therefore a fair approximation to the extinction factor, and can be easily incorporated in a refinement program.

Comparison with a perfect plate in Laue geometry

It is interesting to compare the extinction factor for a sphere and a parallel plate of thickness l in transmission geometry (Fig. 7).

Let a and x be

$$a = \chi l (\cos \alpha_0 \cos \alpha_h)^{-1/2}, \quad x = \chi l. \quad (17)$$

A simple calculation gives

$$y = a^{-1} \int_0^a J_0(2u) du = \int_0^1 J_0(2at) dt. \quad (18)$$

In Fig. 8(a), we plot xy as a function of x , for various Bragg angles, and for a symmetric case: $\alpha_0 =$

$\alpha_h = \theta$. For comparison, we plot (xy_p) for a sphere, for various values of the scattering angle (Fig. 8b).

It is apparent that the amplitude of the oscillations is strongly reduced in the case of a sphere, a consequence of the complicated boundary conditions for an incident plane wave.

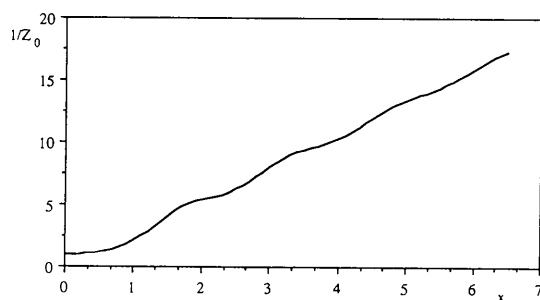
Comparison with Becker-Coppens approximation

Becker & Coppens (1974) proposed an approximation for the primary extinction in a spherical block, based of course on intensity coupling, and therefore physically questionable. For two values of $\sin \theta$, we compare in Fig. 9 $1/y_p$ with $1/y_{BC}$, where y_{BC} is the Becker-Coppens approximation. We observe that the oscillations are absent from y_{BC} , but that the average slope is correct. $|(y_p - y_{BC})/y_p|$ can be of the order of

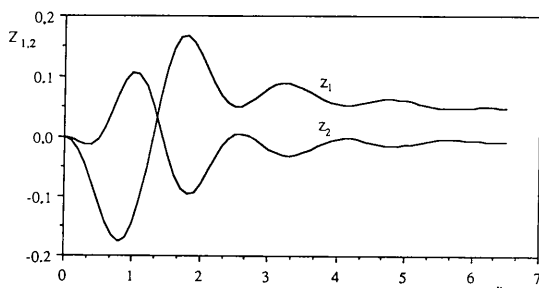
10 to 15% for some values of x . The correctness of the average slope of y_{BC} is certainly one of the reasons for the success of the Becker-Coppens correction for many types of crystals.

Accurate solution for the scattered amplitude in a finite crystal

To improve on the Laue approximation implies the necessity to consider configurations II and III of Fig. 3. An explicit description of the intersection between the parallelogram $SmMm'$ and the crystal surface is needed. The explicit solution can be obtained if this intersection is approximated by a sequence of segments respectively parallel to the incident and the scattered directions.



(a)



(b)

Fig. 6. (a) $1/Z_0(x)$; (b) $Z_1(x)$, $Z_2(x)$.

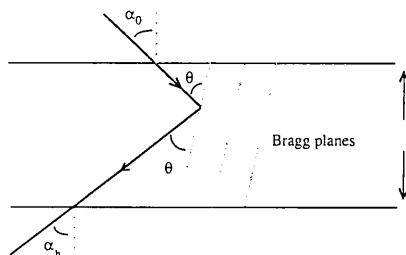
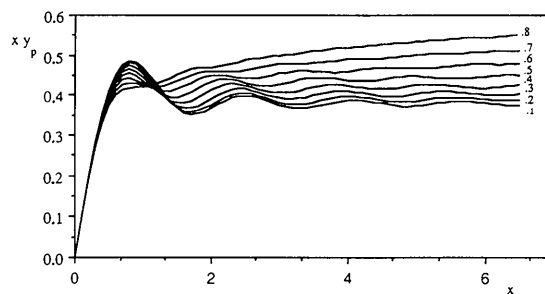
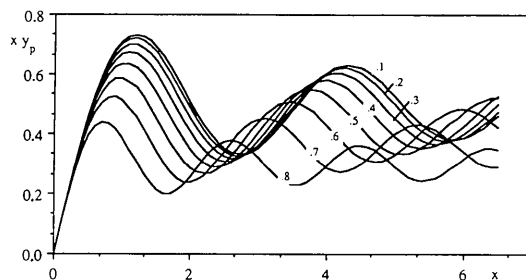


Fig. 7. A parallel plate in transmission geometry: $\alpha_0 + \alpha_h = 2\theta$.



(a)



(b)

Fig. 8. (a) $xy_p(x)$ for a plate, for different values of $\sin \theta$; (b) $xy_p(x)$ for a sphere, for different values of $\sin \theta$.

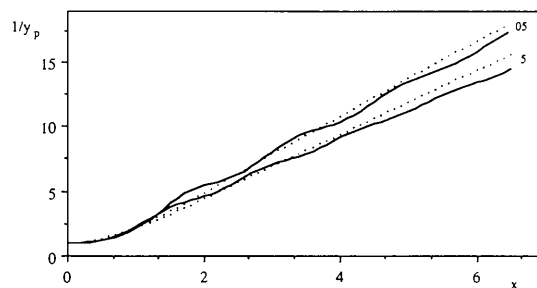


Fig. 9. — $1/y_p(x)$; $\cdots \cdots 1/y_{BC}(x)$ for two values of $\sin \theta$. y_{BC} is based on a Lorentzian shape for the rocking curve.

Configuration II

This configuration is represented in Fig. 10, where the crystal surface CAB is approximated by any number of steps, respectively parallel to s_0 and s_h .

We define the following lengths:

$$c_1 = \overline{mm_1} = \overline{Sn_1}, \quad c_2 = \overline{mm_2} = \overline{Sn_2};$$

$$b_1 = \overline{n_1p_1}, \quad b_2 = \overline{n_2p_2}.$$

The amplitude $D_h(M)$ is calculated by an iteration procedure and involves the values of the amplitudes $D_0(M_i)$ and $D_h(M_i)$ at all points m_i inside the shaded domain of Fig. 10.

By calculations similar to those developed by Becker & Dunstetter (1984), one finds: for $M_1(x, y)$ in domain 1,

$$D_h^1(x, y) = i\chi J_0[2\chi(xy)^{1/2}];$$

for $M_2(x, y)$ in domain 2,

$$D_h^2(x, y) = D_h^1(x, c_1) - \chi \int_{b_1}^x [(y - c_1)/(x - u)]^{1/2} \\ \times J_1\{2\chi[(x - u)(y - c_1)]^{1/2}\} \\ \times D_h^1(u, c_1) du; \quad (19)$$

for $M_n(x, y)$ in domain n ,

$$D_h^n(x, y) = D_h^{n-1}(x, c_{n-1}) \\ - \chi \int_{b_{n-1}}^x [(y - c_{n-1})/(x - u)]^{1/2} \\ \times J_1\{2\chi[(x - u)(y - c_{n-1})]^{1/2}\} \\ \times D_h^{n-1}(u, c_{n-1}) du. \quad (19')$$

Configuration III

Configuration III is depicted in Fig. 11, in parallel to situation II. If

$$c_1 = \overline{n_1p_1}, \quad c_2 = \overline{n_2p_2};$$

$$b_1 = \overline{m'm'_1}, \quad b_2 = \overline{m'm'_2},$$

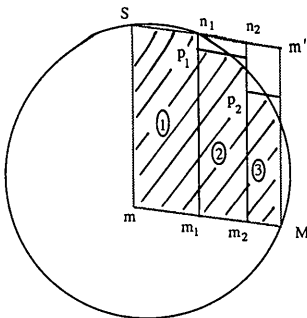


Fig. 10. Geometry associated with configuration II.

one obtains:

for M_1 in domain 1,

$$D_0^1(x, y) = i\chi J_0[2\chi(xy)^{1/2}];$$

for M_2 in domain 2,

$$D_0^2(x, y) = D_0^1(b_1, y) - \chi \int_{c_1}^y [(x - b_1)/(y - v)]^{1/2} \\ \times J_1\{2\chi[(x - b_1)(y - v)]^{1/2}\} \\ \times D_0^1(b_1, v) dv \quad (20)$$

for M_n in domain n ,

$$D_0^n(x, y) = D_0^{n-1}(b_{n-1}, y) \\ - \chi \int_{c_{n-1}}^y [(x - b_{n-1})/(y - v)]^{1/2} \\ \times J_1\{2\chi[(x - b_{n-1})(y - v)]^{1/2}\} \\ \times D_0^{n-1}(b_{n-1}, v) dv \quad (20')$$

and

$$D_h^n = (1/i\chi)\partial D_0^n/\partial x$$

is finally given as

$$D_h^n(x, y) = i\chi \int_{c_n}^y J_0\{2\chi[(x - b_n)(y - v)]^{1/2}\} \\ \times D_0^{n-1}(b_n, v) dv. \quad (21)$$

The expressions (19)–(21) can be used for any finite crystal of convex shape. We will apply them now to the case of an isotropic crystal, approximated by a sphere.

Accurate extinction factor for a perfect sphere

We wish to apply the previous expressions for the amplitude to the case of a perfect sphere. It is possible to separate the domain into three regions I, II, III, each corresponding to one of the fundamental configurations discussed above (Fig. 12). The surface (Σ) which separates I from II is the locus of points m such that point m' of $SmMm'$ lies on the crystal surface.

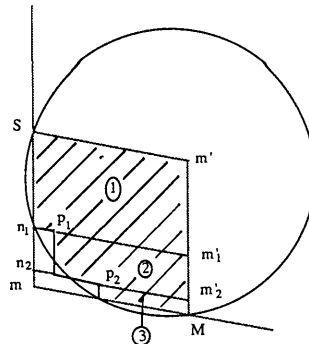


Fig. 11. Geometry for configuration III.

Let v_1, v_2, v_3 be the three volumes associated with these regions. The extinction factor is

$$y(x, \theta) = (3/4\pi\chi^2) \left[\int_{v_1} |D_h(\text{I})|^2 dv + \int_{v_2} |D_h(\text{II})|^2 c v + \int_{v_3} |D_h(\text{III})|^2 dv \right], \quad (22)$$

where $D_h(i)$ is the appropriate expression for configuration i .

Let us, for example, choose a point m in the region II: Fig. 13. We propose the following procedure.

We take q_2 such that $m'q_2 = q_2n_2$. First we consider the boundary $n_1p_1rp_2n_2$, which leads to an amplitude

$D_h(\text{II}, 1)$ and then the boundary $n_1q_1rq_2n_2$, leading to an amplitude $D_h(\text{II}, 2)$. The intensity $I_h(m)$ is approximated by

$$I_h(m) = \frac{1}{4} |D_h(\text{II}, 1) + D_h(\text{II}, 2)|^2. \quad (23)$$

A similar procedure is repeated with three steps rather than two, then four, . . . , n steps.

The convergence test which is chosen is the following. At step n let

$$\Delta_n = \frac{1}{2} [|D_h^n(\text{II}, 1)|^2 + |D_h^n(\text{II}, 2)|^2 - |D_h^n(\text{II}, 1) + D_h^n(\text{II}, 2)|^2] = \frac{1}{4} |D_h^n(\text{II}, 1) - D_h^n(\text{II}, 2)|^2. \quad (24)$$

We stop when Δ_n becomes smaller than a given value ε : in practice we adopted $\varepsilon = 2 \times 10^{-4}$ here.

The same procedure can of course be adopted when m belongs to III.

By this technique, it is possible to obtain a very precise value for the extinction factor. In what follows, we will call the result $y_{AB}(x, \theta)$. $1/y_{AB}$ is plotted versus x , for various $\sin \theta$ values, in Fig. 14, and numerical values are given in Table 3.

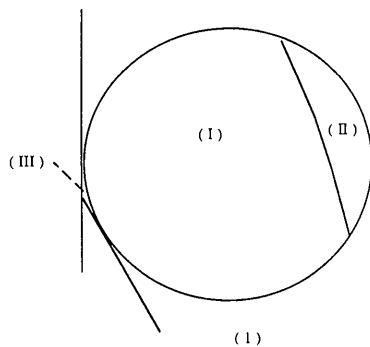


Fig. 12. The three regions corresponding to well defined configurations for the calculation of the diffracted amplitude, in the case of a sphere.

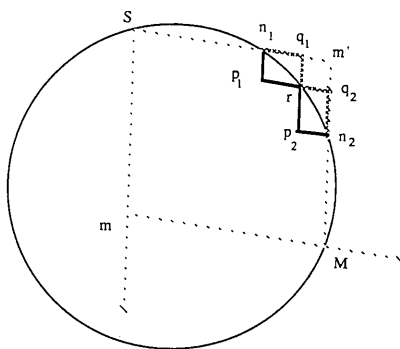


Fig. 13. Geometrical decomposition for a point m in region II.

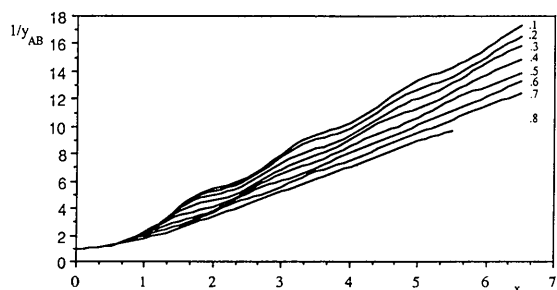


Fig. 14. $1/y_{AB}$ versus x , for different $\sin \theta$ values.

Kawamura and Kato's approximations

Kawamura & Kato (1983) proposed another method, more approximate but simple. This method is summarized in Fig. 15.

They first approximated the boundary by the straight line n_1n_2 , then by the tangent $n'_1n'_2$ parallel to n_1n_2 , and finally by an intermediate line pq such that the area of $(SpqMmS)$ is equal to the exact area limited by the crystal. We call the extinction correction for this approximation $y_K(x, \theta)$. The expressions for the amplitudes are given in the Appendix.

Practical expressions for y

For y_{AB} and y_K , we adopt the same fitting procedure as the one used for the Laue approximation y_p .

By least-squares adjustment we write

$$y_{AB} \approx Z'_0(x) + Z'_1(x) \sin^2(\theta) + Z'_2(x) \sin^4(\theta) \quad (25)$$

$$y_K \approx Z''_0(x) + Z''_1(x) \sin^2(\theta) + Z''_2(x) \sin^4(\theta).$$

The resulting functions Z'_i are shown in Fig. 16, and compared with Z_i for the Laue approximation. Those functions are also given in Table 4.

We observe that $Z_0 \sim Z'_0 \sim Z''_0$, as expected, since it corresponds to the limit $\theta \sim 0$ (pure Laue). However, the functions Z'_1 and Z'_2 , for example, are quite different from Z_1 since the corrections from the Laue situation are of increasing importance when the Bragg angle is larger. y_{AB} is the most precise solution, but for most experimental situations, y_p is a reasonable and simple approximation.

Table 3. y_{AB} as a function of x and $\sin \theta$

$\sin \theta$	0.05	0.1	0.2	0.3	0.4	0.5	0.6	0.7	0.8
X									
0.0	1.0000	1.0000	1.0000	1.0000	1.0000	1.0000	1.0000	1.0000	1.0000
0.1	0.9920	0.9920	0.9918	0.9915	0.9912	0.9907	0.9903	0.9901	0.9907
0.2	0.9685	0.9683	0.9677	0.9666	0.9652	0.9635	0.9618	0.9613	0.9637
0.3	0.9306	0.9303	0.9289	0.9267	0.9236	0.9201	0.9169	0.9162	0.9210
0.4	0.8803	0.8797	0.8775	0.8738	0.8689	0.8633	0.8587	0.8581	0.8678
0.5	0.8199	0.8191	0.8160	0.8109	0.8041	0.7969	0.7913	0.7924	0.8095
0.6	0.7524	0.7514	0.7475	0.7411	0.7329	0.7245	0.7193	0.7242	0.7506
0.7	0.6807	0.6796	0.6750	0.6677	0.6587	0.6504	0.6473	0.6579	0.6947
0.8	0.6080	0.6067	0.6018	0.5941	0.5852	0.5783	0.5791	0.5971	0.6438
0.9	0.5369	0.5356	0.5307	0.5232	0.5155	0.5113	0.5176	0.5438	0.5985
1.0	0.4699	0.4687	0.4641	0.4576	0.4520	0.4519	0.4649	0.4989	0.5582
1.1	0.4090	0.4080	0.4041	0.3992	0.3964	0.4015	0.4216	0.4619	0.5216
1.2	0.3556	0.3548	0.3519	0.3490	0.3499	0.3606	0.3873	0.4316	0.4876
1.3	0.3103	0.3098	0.3081	0.3076	0.3125	0.3287	0.3609	0.4063	0.4553
1.4	0.2734	0.2732	0.2728	0.2748	0.2837	0.3050	0.3408	0.3840	0.4245
1.5	0.2444	0.2445	0.2455	0.2499	0.2625	0.2878	0.3251	0.3633	0.3954
1.6	0.2226	0.2230	0.2252	0.2319	0.2475	0.2754	0.3118	0.3432	0.3686
1.7	0.2069	0.2075	0.2107	0.2192	0.2371	0.2660	0.2994	0.3232	0.3446
1.8	0.1959	0.1967	0.2007	0.2105	0.2297	0.2582	0.2869	0.3036	0.3236
1.9	0.1883	0.1892	0.1937	0.2043	0.2239	0.2506	0.2737	0.2848	0.3057
2.0	0.1829	0.1839	0.1886	0.1994	0.2186	0.2425	0.2598	0.2674	0.2902
2.1	0.1786	0.1796	0.1842	0.1948	0.2130	0.2334	0.2454	0.2519	0.2768
2.2	0.1746	0.1754	0.1798	0.1899	0.2066	0.2234	0.2312	0.2388	0.2645
2.3	0.1701	0.1709	0.1749	0.1843	0.1992	0.2126	0.2177	0.2278	0.2528
2.4	0.1650	0.1657	0.1692	0.1779	0.1911	0.2015	0.2056	0.2189	0.2415
2.5	0.1591	0.1596	0.1628	0.1708	0.1825	0.1908	0.1951	0.2114	0.2307
2.6	0.1525	0.1529	0.1558	0.1633	0.1739	0.1807	0.1864	0.2048	0.2205
2.7	0.1454	0.1458	0.1485	0.1557	0.1655	0.1717	0.1795	0.1985	0.2111
2.8	0.1383	0.1387	0.1413	0.1485	0.1579	0.1639	0.1739	0.1920	0.2031
2.9	0.1314	0.1318	0.1346	0.1419	0.1511	0.1575	0.1693	0.1854	0.1960
3.0	0.1251	0.1255	0.1285	0.1361	0.1453	0.1522	0.1652	0.1785	0.1895
3.1	0.1194	0.1199	0.1232	0.1313	0.1404	0.1478	0.1613	0.1716	0.1842
3.2	0.1147	0.1153	0.1189	0.1273	0.1364	0.1441	0.1573	0.1649	0.1790
3.3	0.1108	0.1115	0.1154	0.1241	0.1329	0.1407	0.1530	0.1589	0.1737
3.4	0.1078	0.1085	0.1127	0.1215	0.1298	0.1374	0.1484	0.1535	0.1683
3.5	0.1054	0.1061	0.1105	0.1192	0.1268	0.1340	0.1436	0.1489	0.1632
3.6	0.1034	0.1042	0.1087	0.1170	0.1237	0.1305	0.1388	0.1451	0.1581
3.7	0.1017	0.1025	0.1069	0.1148	0.1205	0.1268	0.1342	0.1418	0.1532
3.8	0.1001	0.1008	0.1051	0.1124	0.1172	0.1232	0.1299	0.1386	0.1487
3.9	0.0984	0.0991	0.1031	0.1097	0.1137	0.1196	0.1260	0.1358	0.1449
4.0	0.0964	0.0970	0.1009	0.1068	0.1101	0.1162	0.1225	0.1327	0.1413
4.1	0.0942	0.0948	0.0984	0.1037	0.1067	0.1131	0.1197	0.1296	0.1380
4.2	0.0918	0.0923	0.0957	0.1005	0.1034	0.1103	0.1171	0.1262	0.1347
4.3	0.0892	0.0897	0.0930	0.0974	0.1004	0.1078	0.1148	0.1227	0.1313
4.4	0.0865	0.0870	0.0902	0.0944	0.0978	0.1056	0.1125	0.1194	0.1283
4.5	0.0839	0.0844	0.0876	0.0917	0.0956	0.1036	0.1102	0.1162	0.1251
4.6	0.0814	0.0819	0.0853	0.0894	0.0938	0.1017	0.1078	0.1132	0.1219
4.7	0.0792	0.0797	0.0832	0.0873	0.0922	0.0998	0.1055	0.1107	0.1188
4.8	0.0772	0.0778	0.0814	0.0856	0.0908	0.0978	0.1031	0.1083	0.1161
4.9	0.0756	0.0762	0.0799	0.0841	0.0895	0.0958	0.1009	0.1063	0.1138
5.0	0.0742	0.0748	0.0786	0.0828	0.0882	0.0937	0.0986	0.1046	0.1116
5.1	0.0730	0.0737	0.0775	0.0815	0.0868	0.0915	0.0965	0.1026	0.1096
5.2	0.0721	0.0727	0.0765	0.0803	0.0853	0.0893	0.0947	0.1008	0.1078
5.3	0.0712	0.0718	0.0755	0.0790	0.0836	0.0872	0.0930	0.0989	0.1062
5.4	0.0703	0.0709	0.0744	0.0776	0.0819	0.0853	0.0914	0.0970	0.1043
5.5	0.0693	0.0699	0.0733	0.0760	0.0801	0.0835	0.0898	0.0951	0.1028
5.6	0.0683	0.0688	0.0720	0.0745	0.0783	0.0820	0.0883	0.0931	
5.7	0.0671	0.0676	0.0706	0.0728	0.0766	0.0806	0.0868	0.0913	
5.8	0.0658	0.0663	0.0691	0.0712	0.0750	0.0794	0.0851	0.0895	
5.9	0.0645	0.0650	0.0676	0.0697	0.0736	0.0784	0.0836	0.0880	
6.0	0.0631	0.0636	0.0662	0.0683	0.0723	0.0774	0.0820	0.0865	
6.1	0.0618	0.0622	0.0648	0.0670	0.0711	0.0764	0.0805	0.0855	
6.2	0.0605	0.0609	0.0635	0.0659	0.0701	0.0753	0.0790	0.0843	
6.3	0.0593	0.0598	0.0624	0.0649	0.0691	0.0742	0.0777	0.0834	
6.4	0.0582	0.0587	0.0614	0.0640	0.0682	0.0730	0.0764	0.0826	
6.5	0.0573	0.0579	0.0606	0.0632	0.0672	0.0718	0.0753	0.0818	

Concluding remarks

It has been shown that we can approach very closely the exact dynamical results for a finite perfect crystal. For a sphere, the extinction correction is $y(x, \sin \theta)$ where $x = R/\Lambda$, R being the radius of the crystal and $\Lambda = 1/\chi$ the extinction length. Besides numerical calculation, it has been shown that, to an accuracy of at least 1%, y can be represented by the expression

$$y(x, \sin \theta) \approx Z_0(x) + \sin^2(\theta) Z_1(x) + \sin^4(\theta) Z_2(x),$$

where the $Z_i(x)$ are to be considered as numerical functions. This semi-analytical form is very well suited for applications in refinement procedures. We intend, in a forthcoming paper, to propose a similar expansion of the extinction factor for real crystals.

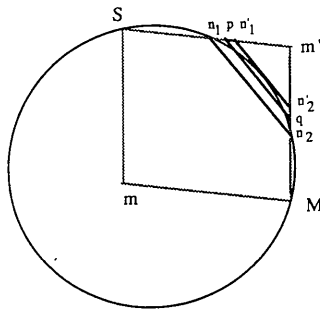
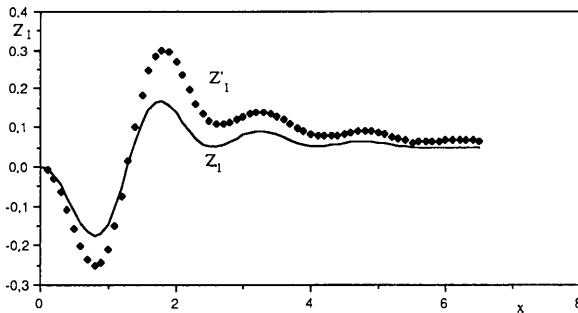
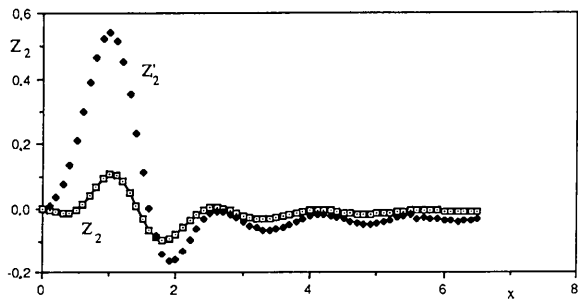


Fig. 15. Kawamura & Kato's geometrical approximation.



(a)



(b)

Fig. 16. (a) Z_1, Z_1' ; (b) Z_2, Z_2' .

APPENDIX

The geometry adopted by Kawamura & Kato (1983) is depicted in Figs. 17 and 18.

Configuration II

The geometry is shown in Fig. 17, where the intersection between $SmMm'$ and the crystal is approximated by a straight line: n_1n_2 .

The domain to be considered for scattering from S to M is divided into two regions. Let $c = Sn_1$, $\beta_0 = \sin \alpha_0$, $\beta_h = \sin \alpha_h$.

By using the same procedure as that used by Kawamura & Kato (1983) and Becker & Dunstetter (1984), one finds:

for M_1 in domain 1,

$$D_h^1(x, y) = i\chi J_0[2\chi(xy)^{1/2}];$$

for M_2 in domain 2,

$$D_h^2(x, y) = D_h^1(x, y) - i\chi(\beta_h/\beta_0)\{(y-c)/x + (\beta_h/\beta_0)c\} \times J_2[2\chi\{(y-c)[x + (\beta_h/\beta_0)c]\}^{1/2}]. \quad (A1)$$

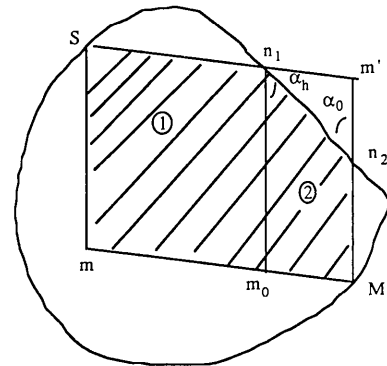


Fig. 17. Kawamura & Kato's approximation of configuration II geometry.

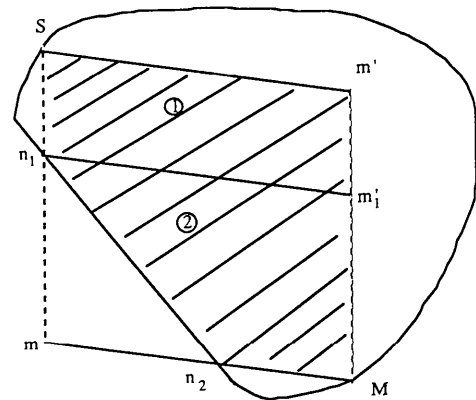


Fig. 18. Kawamura & Kato's approximation of configuration III geometry.

EXTINCTION IN FINITE PERFECT CRYSTALS

Table 4. Z'_0, Z'_1, Z'_2 as functions of x and Z''_0, Z''_1, Z''_2 as functions of x

x	Z'_0	Z'_1	Z'_2	x	Z'_0	Z'_1	Z'_2
0.0	1.0000	0.0000	0.0000	3.3	0.1109	0.1369	-0.0645
0.1	0.9921	-0.0081	0.0090	3.4	0.1082	0.1333	-0.0663
0.2	0.9689	-0.0317	0.0359	3.5	0.1061	0.1263	-0.0630
0.3	0.9314	-0.0659	0.0760	3.6	0.1044	0.1176	-0.0570
0.4	0.8815	-0.1098	0.1349	3.7	0.1028	0.1080	-0.0490
0.5	0.8218	-0.1571	0.2110	3.8	0.1011	0.0984	-0.0400
0.6	0.7548	-0.2017	0.2994	3.9	0.0993	0.0891	-0.0292
0.7	0.6834	-0.2350	0.3889	4.	0.0972	0.0821	-0.0211
0.8	0.6106	-0.2504	0.4673	4.1	0.0948	0.0782	-0.0168
0.9	0.5391	-0.2429	0.5218	4.2	0.0922	0.0766	-0.0159
1.	0.4711	-0.2093	0.5398	4.3	0.0894	0.0776	-0.0192
1.1	0.4089	-0.1515	0.5161	4.4	0.0866	0.0799	-0.0236
1.2	0.3539	-0.0747	0.4514	4.5	0.0839	0.0830	-0.0303
1.3	0.3069	0.0133	0.3531	4.6	0.0815	0.0861	-0.0375
1.4	0.2686	0.1024	0.2344	4.7	0.0793	0.0886	-0.0439
1.5	0.2386	0.1830	0.1110	4.8	0.0775	0.0888	-0.0466
1.6	0.2164	0.2456	0.0000	4.9	0.0760	0.0875	-0.0466
1.7	0.2009	0.2850	-0.0860	5.	0.0748	0.0848	-0.0444
1.8	0.1907	0.3006	-0.1414	5.1	0.0737	0.0801	-0.0394
1.9	0.1842	0.2937	-0.1637	5.2	0.0729	0.0749	-0.0333
2.	0.1802	0.2697	-0.1586	5.3	0.0720	0.0692	-0.0261
2.1	0.1772	0.2345	-0.1323	5.4	0.0710	0.0650	-0.0215
2.2	0.1742	0.1968	-0.0973	5.5	0.0700	0.0604	-0.0155
2.3	0.1704	0.1617	-0.0613	5.6	0.0686	0.0643	-0.0291
2.4	0.1656	0.1342	-0.0321	5.7	0.0673	0.0627	-0.0276
2.5	0.1596	0.1165	-0.0133	5.8	0.0659	0.0626	-0.0289
2.6	0.1527	0.1083	-0.0056	5.9	0.0645	0.0636	-0.0313
2.7	0.1453	0.1086	-0.0084	6.	0.0631	0.0652	-0.0351
2.8	0.1378	0.1128	-0.0154	6.1	0.0617	0.0657	-0.0353
2.9	0.1307	0.1206	-0.0274	6.2	0.0604	0.0668	-0.0376
3.	0.1244	0.1285	-0.0409	6.3	0.0593	0.0664	-0.0366
3.1	0.1189	0.1341	-0.0509	6.4	0.0583	0.0654	-0.0341
3.2	0.1144	0.1368	-0.0589	6.5	0.0576	0.0628	-0.0293

x	Z''_0	Z''_1	Z''_2	x	Z''_0	Z''_1	Z''_2
0.0	1.0000	0.0000	0.0000	3.3	0.1096	0.1005	0.1533
0.1	0.9919	-0.0030	-0.0121	3.4	0.1071	0.1002	0.1487
0.2	0.9682	-0.0119	-0.0449	3.5	0.1051	0.0968	0.1477
0.3	0.9301	-0.0291	-0.0847	3.6	0.1034	0.0912	0.1501
0.4	0.8798	-0.0552	-0.1158	3.7	0.1018	0.0844	0.1551
0.5	0.8198	-0.0908	-0.1216	3.8	0.1002	0.0779	0.1605
0.6	0.7530	-0.1338	-0.0915	3.9	0.0983	0.0727	0.1652
0.7	0.6825	-0.1792	-0.0243	4.	0.0960	0.0700	0.1675
0.8	0.6110	-0.2206	0.0732	4.1	0.0935	0.0690	0.1677
0.9	0.5411	-0.2513	0.1872	4.2	0.0907	0.0713	0.1632
1.	0.475	-0.2644	0.2982	4.3	0.0878	0.0755	0.1560
1.1	0.4144	-0.2551	0.3866	4.4	0.0850	0.0804	0.1473
1.2	0.3606	-0.2229	0.4395	4.5	0.0823	0.0864	0.1364
1.3	0.3144	-0.1715	0.4518	4.6	0.0798	0.0915	0.1265
1.4	0.2762	-0.1071	0.4253	4.7	0.0777	0.0952	0.1185
1.5	0.2460	-0.0401	0.3724	4.8	0.0759	0.0970	0.1134
1.6	0.2231	0.0211	0.3069	4.9	0.0745	0.0966	0.1113
1.7	0.2067	0.0687	0.2439	5.	0.0734	0.0947	0.1112
1.8	0.1955	0.0976	0.1965	5.1	0.0725	0.0911	0.1138
1.9	0.1883	0.1069	0.1715	5.2	0.0716	0.0876	0.1159
2.	0.1836	0.0996	0.1691	5.3	0.0707	0.0840	0.1182
2.1	0.1800	0.0811	0.1849	5.4	0.0697	0.0820	0.1184
2.2	0.1766	0.0572	0.2119	5.5	0.0685	0.0812	0.1165
2.3	0.1724	0.0346	0.2406	5.6	0.0673	0.0807	0.1149
2.4	0.1671	0.0189	0.2626	5.7	0.0659	0.0810	0.1111
2.5	0.1607	0.0118	0.2745	5.8	0.0644	0.0834	0.1068
2.6	0.1533	0.0141	0.2743	5.9	0.0629	0.0853	0.1030
2.7	0.1454	0.0239	0.2638	6.0	0.0615	0.0873	0.0989
2.8	0.1374	0.0398	0.2444	6.1	0.0602	0.0887	0.0958
2.9	0.1299	0.0575	0.2213	6.2	0.0591	0.0892	0.0936
3.	0.1233	0.0736	0.1990	6.3	0.0580	0.0897	0.0913
3.1	0.1176	0.0869	0.1795	6.4	0.0571	0.0890	0.0901
3.2	0.1131	0.0959	0.1641	6.5	0.0564	0.0884	0.0888

The derivation is similar to that of equation (21) of Becker & Dunstetter (1984).

Equation (A2) is obtained in the same way as equation (23) of Becker & Dunstetter (1984).

Configuration III

The geometry of configuration II is shown in Fig. 18 with $b = \overline{S}n_1$. One obtains:
for M_1 in domain 1

$$D_h^1 = i\chi J_0[2\chi(xy)^{1/2}];$$

for M_2 in domain 2,

$$D_h^2(x, y) = D_h^1(x, y) - i\chi \times J_0[2\chi\{(x-b)[y+(\beta_0/\beta_h)b]\}^{1/2}]. \quad (A2)$$

Acta Cryst. (1990). **A46**, 123–129

Diffraction by a Randomly Distorted Crystal. I. The Case of Short-Range Order

BY PIERRE BECKER* AND MOSTAFA AL HADDAD†

*Laboratoire de Cristallographie, associé à l'Université J. Fourier, CNRS, 166X,
38042 Grenoble CEDEX, France*

(Received 28 November 1988; accepted 8 September 1989)

Abstract

Kato's statistical theory of diffraction [Kato (1980). *Acta Cryst.* **A36**, 763–769, 770–778] is reformulated in a self-consistent manner. The local displacement field $\mathbf{u}(\mathbf{r})$ occurs through the phase factor $\varphi(\mathbf{r}) = \exp[2\pi i \mathbf{h} \cdot \mathbf{u}(\mathbf{r})]$. The present paper is concerned with the limiting case where $\langle \varphi(\mathbf{r}) \rangle = E = 0$: this corresponds to the situation where only secondary extinction is present. There are two correlation lengths in the problem, the first one τ for the phase factor φ , the second one Γ for the wave-field amplitudes. Kato assumed $\Gamma \gg \tau$. It is shown in the present paper that $\Gamma \approx \tau$, a property which has important consequences for the general theory, where $E \neq 0$, to be discussed in the second paper of this series.

I. Introduction

Kato (1980a) has proposed a statistical theory that describes the propagation of X-rays and neutrons in

a distorted crystal. This theory covers the whole range of perfection from purely dynamical (perfect crystal) to purely kinematical (mosaic crystal) diffraction. It thus fills the gap between secondary and primary extinction that were treated independently in previous approaches.

The application of this theory has been discussed by Kato (1980b) and an improved solution was recently proposed by the authors (Al Haddad & Becker, 1988) that led to a fair description of experimental data on silicon (Olekhovich, Karpei, Olekhovich & Puzenkova, 1983). This modification was confirmed by Guigay (1989).

The theory involves long-range- and short-range-order parameters. The effective short-range correlation length introduced by Kato has been questioned in the literature (Olekhovich *et al.*, 1983) and relies on non-trivial assumptions.

In this series of papers, we intend to discuss the statistical hypothesis in detail, and to propose an improved self-consistent formulation of the problem. In order to discuss separately the various approximations, we shall start in the present paper by the particular case where long-range order is negligible (secondary extinction only). The general theory will be presented in a second paper, together with a practical solution.

* Present address: Laboratoire de Minéralogie-Cristallographie, Université Pierre et Marie Curie, Tour 16, 4 Place Jussieu, 75252 Paris CEDEX 05, France.

† Present address: Atomic Energy Commission, PO Box 6091, Damascus, Syria.

References

- AL HADDAD, M. & BECKER, P. (1988). *Acta Cryst.* **A44**, 262–270.
BECKER, P. (1977a). *Acta Cryst.* **A33**, 243–249.
BECKER, P. (1977b). *Acta Cryst.* **A33**, 667–671.
BECKER, P. & AL HADDAD, M. (1989). *Acta Cryst.* **A45**, 333–337.
BECKER, P. & AL HADDAD, M. (1990). *Acta Cryst.* **A46**, 123–129.
BECKER, P. & COPPENS, P. (1974). *Acta Cryst.* **A30**, 129–147.
BECKER, P. & COPPENS, P. (1975). *Acta Cryst.* **A42**, 417–425.
BECKER, P. & DUNSTETTER, F. (1984). *Acta Cryst.* **A40**, 241–251.
GUIGAY, J. P. (1989). *Acta Cryst.* **A45**, 241–244.
KATO, N. (1973). *Z. Naturforsch. Teil A*, **28**, 604–609.
KATO, N. (1976). *Acta Cryst.* **A32**, 453–466.
KATO, N. (1980). *Acta Cryst.* **A36**, 763–769, 770–778.
KAWAMURA, T. & KATO, N. (1983). *Acta Cryst.* **A39**, 305–310.